AIMS Biophysics, 3(3): 431-449.
DOI: 10.3934/biophy.2016.3.431
Received: 20 August 2016
Accepted: 22 September 2016
Published: 26 September 2016

http://www.aimspress.com/journal/biophysics

Research article

Re-modeling *Chara* action potential: I. from Thiel model of Ca^{2+} transient to action potential form

Mary Jane Beilby [1,*] and Sabah Al Khazaaly [2]

[1] School of Physics, University of NSW, Kensington, NSW 2052, Australia
[2] Mathematics and Statistics, Western Sydney University, Bankstown, NSW 2200, Australia

* **Correspondence:** E-mail: m.j.beilby@unsw.edu.au.

Abstract: Thiel and colleagues demonstrated that the all-or-none nature of *Chara* action potential (AP) is determined by formation of a second messenger, probably inositol triphosphate (IP_3), which in turn releases Ca^{2+} from internal stores. The Ca^{2+}-activated Cl^- channels are the main agent of the depolarization phase of the AP. Once the Ca^{2+} is re-sequestered by the calcium pumps, the chloride conductance drops and depolarization-activated outward rectifier current, the background current and the proton pump current return the membrane potential difference (PD) to resting level. Departing from the Thiel model of transient increase of Ca^{2+} concentration, we set up membrane PD rate of change equation to calculate the AP form by numerical integration. Compared to data, this model AP depolarized more gradually. We introduced a prompt Ca^{2+} transient from the outside, achieving a good correspondence with the experimental AP. In *Chara* cells subjected to 50 mM NaCl/0.1 mM Ca^{2+} medium, the AP duration increased from 2 s to up to 50 s and the APs were often spontaneous. The lack of stimulating pulse revealed a sharp positive spike at the beginning of each AP, confirming that *Chara* plasma membrane may contain transient receptor potential (TRP)-like channels, possibly activated by another second messenger diacylglycerol (DAG) formed at the same time as IP_3. The long duration of the saline AP can be modeled by decreasing the coefficients in the Hill equation describing the Ca^{2+} pumps on the internal stores. The model provides new insights into the characean AP and suggests a range of experiments.

Keywords: action potential; *Chara*; cytoplasmic Ca^{2+} concentration; Ca^{2+} channels on internal stores; inositol triphosphate; Ca^{2+}-activated Cl^- channels; TRP channels; Ca^{2+} pump

1. Introduction

Hodgkin and Huxley [1] won the Nobel Prize for their description of action potential (AP) in animal kingdom. In the nerve the stimulus depolarization of the membrane potential difference (PD) directly activates Na^+ selective channels, Na^+ inflow further depolarizes the membrane and spontaneous inactivation of the same channels and the outflow of K^+ returns the cell to *status quo* in several ms. Beilby [2] and Beilby and Coster [3,4] fitted the Hodgkin Huxley (HH) equations to AP in giant cells of salt sensitive Characeae *Chara australis,* with the outflow of Cl^- replacing the inflow of Na^+ as the depolarizing ionic flux. In this "green axon" the AP transient takes about 2 s in normal artificial pond water (APW) and at room temperature. Later research found that the Cl^- channels are activated by rise of Ca^{2+} in the cytoplasm [5,6], which in turn may be mediated by inositol 1,4,5-triphosphate (IP_3)-activated Ca^{2+} influx from internal stores [7]. Biskup et al. [8] investigated the effects of inhibitors of IP_3 formation on Cl^- excitation currents in voltage-clamped *Chara* cells. Wacke and Thiel [9] and Wacke et al. [10] measured Ca^{2+} rise in the cytoplasm following a PD stimulus and formulated a new *Chara* AP model, where the threshold, "all-or-none" AP form and refractory period all originate from formation of second messenger (IP_3), opening of the Ca^{2+} channels on internal stores and re-sequestration of the Ca^{2+} by calcium pumps. Interestingly, parts of this model are also "borrowed" from animal cells [11]. Tazawa and Kikuyama [12] were not able to replicate the Thiel experiments: IP_3 did not stimulate excitation, nor did Neomycin and U73122 inhibit it. Future experiments, suggested by the present modelling, will provide more details of this signalling pathway.

The present work was initially inspired by observation of prolonged APs in salt-stressed *Chara*. The modeling departs from the Thiel model of transient Ca^{2+} concentration rise and activation of Cl^- channels to calculate the form of the action potential and compare it to the experimental data under normal conditions and at the time of saline stress. The restoration of the resting PD depends on the drop in cytoplasmic Ca^{2+} concentration and inactivation of the Cl^- current, the outward rectifier current (activated by depolarization), the background current and the proton pump current (Figure 1). The PD dependence of the last three transporters was presumed unchanged by the brief transient Ca^{2+} concentration rise. The effect of salinity stress on the shape of the AP is explored in the terms of the combined Thiel-Beilby model.

2. Materials and Methods

2.1. Materials

The experimental AP data were obtained from *Chara australis*. The "standard" AP, designated "AP_{av}", in APW (NaCl 1 mM, KCl 0.1 mM, $CaCl_2$ 0.1 mM, neutral pH) and at room temperature was adopted from previous AP modeling (see [2] and Results section). To elicit excitation under such conditions a short depolarizing current pulse was applied to the cell. The AP, which displayed slight separation from the excitation pulse, was selected and the pulse was excluded from the data to obtain what was then considered the "pure" AP form.

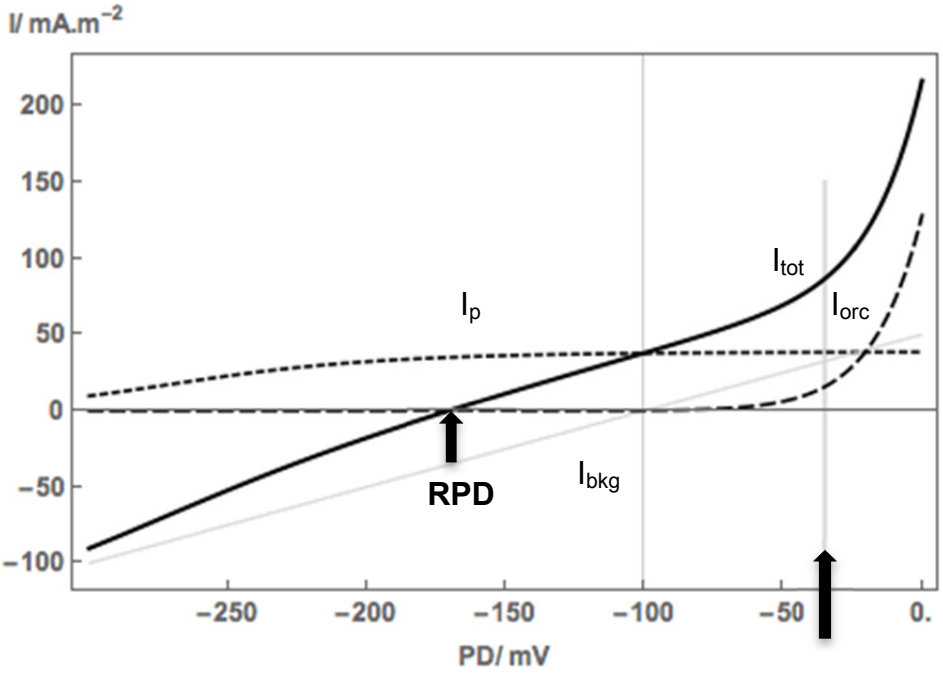

Figure 1. I/V characteristics of the most conductive transporters in *Chara* plasma membrane in APW: the proton pump, I_p, (short-dashed line), the background current, I_{bkg}, (thin gray line), the outward rectifier, I_{orc}, (long-dashed line) and the total current I_{tot} (thick black line). The values of the model parameters were selected to match the resting potential difference, RPD, (see arrow) of the standard experimental AP_{av} (see next section) and can be found in Table 1b. The positive currents near –30 mV (shown as vertical gray line and another arrow) balance the I_{Cl} at the peak of the AP and once the I_{Cl} decreases due to drop in Ca^{2+} concentration, the proton pump current restores the resting PD.

C. australis is salt sensitive and cells die in 5 days in comparatively mild salinity of 50–100 mM NaCl added to APW [13]. Electrophysiology, particularly current-voltage (I/V) scans, add to the cell stress and we often observed loss of cell PD and streaming after a few hours in Saline APW [13,14,15]. The survival of the saline-stressed cells was prolonged by applying the osmotic stress separately and exposing the cell to Sorbitol APW for 1 hr, with sorbitol concentration adjusted to the same osmolarity as the Saline APW with 50 mM NaCl and 0.1 mM Ca^{2+}. The spontaneous APs, designated "AP_{sal}", with prolonged durations were only observed in the Saline APW. Repetitive periodic APs were recorded when the membrane PD depolarized to the excitation threshold of –100 mV. In the investigations of the salinity effect on the cell electrophysiology the membrane PD was continuously data-logged at 0.1 s intervals throughout each experiment and stored as text files. In the present modeling studies the APs were selected from the whole PD record and entered into Mathematica 10 programs.

2.2. The Thiel Model

Zherelova [16] and Thiel et al. [5] elicited APs in *Chara* and *Nitella* by artificial elevation of IP_3 in the cytoplasm. Biskup et al. [8] found that the inhibitors of phospholipase C (PLC), Neomycin and U73122, inhibited excitation in *Chara*. In animal cells IP_3 is cleaved from the membrane bound phosphatidyl inositol 4,5-biphosphate (PIP_2) by PLC. Wacke and Thiel [9] measured cytoplasmic Ca^{2+} concentration as a function of depolarising current pulses. To liberate Ca^{2+} from internal stores, IP_3 had to reach a critical concentration. The spacing of a double pulse provided data about the IP_3 formation and decay into IP_2 and replenishing of the PIP_2 pool.

Following Othmer [11], Wacke et al. [10] modelled the Ca^{2+} channels on the internal stores as transiting between 4 states: unbound (R), bound to IP_3 (IR), bound to IP_3 and activating Ca^{2+} molecule (IRC_+), bound to IP_3 and second inactivating Ca^{2+} molecule (IRC_+C_-). The channel is only conductive in IRC_+ state. The long lifetime of the last state is thought to be responsible for the refractory period.

We can set up rate equations for change in Ca^{2+} cytoplasmic concentration, C, and fractions of channels in each state: x_2 (R), x_3 (IR), x_4 (IRC_+) and x_5 (IRC_+C_-):

$$\begin{aligned} &R + I \xleftarrow{k_1, k_{-1}} RI \\ &RI + C \xleftarrow{k_2, k_{-2}} RIC_+ \\ &RIC_+ + C \xleftarrow{k_3, k_{-3}} RIC_+C_- \end{aligned} \tag{1}$$

The initial chemical stimulus is the appearance of IP_3 in the system, initiated by depolarising current pulse. The concentration of IP_3, I, decays from the initial amount, I_0, with time t [10]:

$$I = I_0 e^{-0.2\,t} \tag{2}$$

Scaled Ca^{2+} concentration:

$$x_1 = \frac{C}{C_0}$$

$$C_0 = \frac{C + \nu_r C_s}{1 + \nu_r} \tag{3a, b}$$

where C_0 = average calcium concentration, C_s = Ca^{2+} concentration in the store, ν_r = ratio of endoplasmic reticulum (ER) volume to cytoplasmic volume.

$$\frac{dx_1}{dt} = \lambda(\gamma_0 + \gamma_1 x_4)(1 - x_1) - \frac{p_1 x_1^4}{p_2^4 + x_1^4} \tag{4}$$

where γ_0 = permeability of Ca^{2+} store in absence of IP_3, γ_1 = density of IP_3 activated channels, $\lambda = 1 + \nu_r$. The last ratio in the equation (4) is the Hill function, which describes the calcium conductance of the Ca^{2+} pump with scaled Hill coefficients $p_1 = p'_1/C_0$ and $p_2 = p'_2/C_0$ [11].

$$\frac{dx_2}{dt} = -k_1 I x_2 + k_{-1} x_3 \quad (5)$$

$$\frac{dx_3}{dt} = -(k_{-1} + k_2 x_1) x_3 + k_1 I x_2 + k_{-2} x_4 \quad (6)$$

$$\frac{dx_4}{dt} = k_2 x_1 x_3 + k_{-3} x_5 - (k_{-2} + k_3 x_1) x_4 \quad (7)$$

$$\frac{dx_5}{dt} = k_3 x_1 x_4 - k_{-3} x_5 \quad (8)$$

where k_i ($i = \pm 1, \pm 2, \pm 3$) are the rate constants for forward and backward transitions between the channel states (see equation 1). Some of the rate constants are also scaled by C_0: $k_2 = k'_2 C_0$ and $k_3 = k'_3 C_0$. With the scaling, all x_i range between 0 and 1. As the channels have to be in one of the four states, conservation condition applies: $\Sigma_{k=2}^{5} x_k = 1$. Wacke et al. [10] started with parameter values used by Othmer [11] and gradually modified some of them to suit *Chara* Ca^{2+} concentration data (see Table 1a).

To re-construct the transient increase in cytoplasmic Ca^{2+} the Thiel model was programmed into Mathematica 10. The numerical integration of equations (4)–(8) was performed by three concentric DO-loops, one to apply 4th order Runge-Kutta method, the second to advance time and the third to test different time intervals and parameter values. In this study, we are not interested in the stimulus properties, so the excitation was initiated by introducing the initial IP_3 concentration, I_0, into the model (equation 2). We tested different IP_3 concentrations, I_0, and selected 2.5 μM for saturating Ca^{2+} concentration increase (see Figure 4 of Wacke et al. [10]) and a shorter delay before the steep Ca^{2+} concentration rise (Figure 2). The changes to Thiel model parameters are summarized in Table 1a. The programs can be found on MJ Beilby website link "Action Potential models": http://newt.phys.unsw.edu.au/~mjb/APproj.html.

2.3. The Thiel-Beilby Model

To calculate the PD transient we start from the rate of change of the membrane PD, V:

$$\frac{dV}{dt} = -\frac{1}{C_m}\left[\frac{G_{Cl,max}(V - E_{Cl})}{\left(1 + \frac{k_i}{k_a x_1}\right)} + I_p + I_{orc} + I_{bkg} + I_{TRP,Ca}\right] \quad (9)$$

where C_m is the membrane capacitance (Table 1b) and the terms inside the square bracket are all the currents flowing at the time of the AP. The first ratio in the square brackets is the Ca^{2+}-activated chloride current, I_{Cl}. This model was formulated by Biskup et al. [8] and fitted to excitation voltage clamp currents. The rate constants k_a and k_i describe the activation and inactivation of I_{Cl} by

increased Ca^{2+} concentration in the cytoplasm (Table 1a). $G_{Cl,max}$ was set in range suggested by previous modeling ([2,4] and Table 1b).

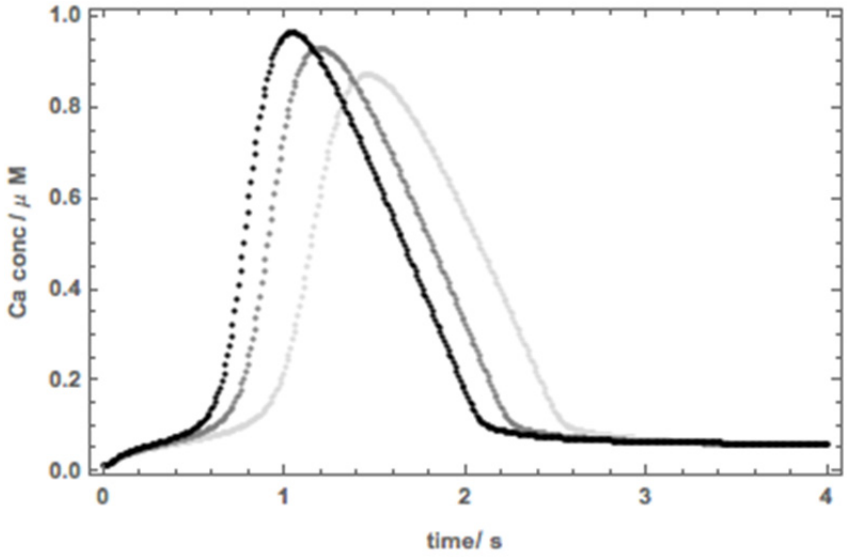

Figure 2. The output from our reconstructed Thiel model for Ca^{2+} concentration transient. Excitation was triggered by initial concentrations of IP_3, I_0: 1μM (light gray), 1.5 μM (gray), 2.5 μM (black). The other parameters can be found in Table 1a.

The proton pump current, I_p, the background current, I_{bkg}, and the outward rectifier current, I_{orc}, are part of the electrophysiological make up of the *Chara* plasma membrane (Figure 1 and Chapter 2 of Beilby and Casanova [17] for the full description of the modeling of I/V characteristics of these transporters). It is assumed that the brief increase in the cytoplasmic Ca^{2+} concentration does not influence the PD dependencies of these transporters.

Briefly: The PD dependence of I_p is calculated from HGSS (Hansen, Gradmann, Sanders and Slayman) single cycle two state model, based on cyclic enzyme-mediated transport [18]. The voltage-independent steps, such as ATP-, ADP-, inorganic phosphate- and H^+ binding and de-binding steps and carrier recycling, are represented by rate constants κ_{io} and κ_{oi}, while the charge transit is characterised by the rate constants k_{io} and $k_{oi,}$ across a symmetrical Eyring barrier.
The dependence of the pump current, I_p, on membrane PD, V, is given by:

$$I_p = z_p F N \frac{k_{io}\kappa_{oi} - k_{oi}\kappa_{io}}{k_{io} + k_{oi} + \kappa_{io} + \kappa_{oi}} \tag{10}$$

$$k_{io} = k_{io}^0 e^{\frac{z_p FV}{2RT}}$$

$$k_{oi} = k_{oi}^0 e^{-\frac{z_p FV}{2RT}} \tag{11a, b}$$

Table 1a. Thiel model parameters and Beilby modifications. Blank compartments mean that the same parameters were used in both models.

Parameter	Thiel model	Thiel-Beilby model		
		AP_{av}	$AP_{av,\ hyper}$	AP_{sal}
ν_r	0.185			
γ_0	0.1 s^{-1}			
γ_1	20.5 s^{-1}			
p_1,	8.5 μM.s^{-1}	8 μM.s^{-1}		1.59 (1.5) μM.s^{-1} (Fig. 5b)
				1.3 μM.s^{-1} (Fig. 6a, AP 1)
				0.9 μM.s^{-1} (Fig. 6a, AP 2)
				0.75 μM.s^{-1} (Fig. 6a, AP 3)
				0.66 μM.s^{-1} (Fig. 6a, AP 4)
p_2,	0.065 μM	0.035 μM		0.009 (0.0125) μM (Fig. 5b)
				0.013 μM (Fig. 6a, AP 1)
				0.01 μM (Fig.6a, AP 2)
				0.0075 μM (Fig. 6a, AP 3)
				0.0069 μM (Fig. 6a, AP 4)
C_0	1.56 μM			
k_1	12.0 (μM.s)$^{-1}$			
k_{-1}	8.0 s^{-1}			
k_2'	15.0 (μM.s)$^{-1}$			
k_{-2}	1.65 s^{-1}			
k_3'	1.8 (μM.s)$^{-1}$			
k_{-3}	0.04 s^{-1}			
IP_3	0.01–10 μM	2.5 μM		0.5, 2.5 μM (Fig. 5b)
				2.5 μM (Fig. 6a)
k_a	2 s^{-1}			
k_i	2 s^{-1}			
ΔCa^{2+} (period of application)		0.0355 (0.04–0.16 s)	0.02 (0.04–0.13 s)	0.035 (Fig. 5b) (0.04–0.16 s)
				0.035 (Fig. 6a) (0.04–0.16 s)

Table 1b. Thiel-Beilby model parameters for the membrane transporters.

Parameter	AP_{av}	$AP_{av\ hyper}$	AP_{sal}
		Proton pump I_p	
κ_{oi}	22 s^{-1}	140 s^{-1}	140 s^{-1} (Fig. 5b)
			50 s^{-1} (Fig. 6a)
k_{io}^0	6000 s^{-1}	7000 s^{-1}	7000 s^{-1} (Fig. 5b)
			6000 s^{-1} (Fig. 6a)
k_{oi}^0	0.1 s^{-1}		
κ_{io}	0.1 s^{-1}		
		Background current I_{bkg}	
G_{bkg}	0.5 $S.m^{-2}$		0.5 (Fig. 5b)
			1.6 (Fig. 6a)
		Outward rectifier I_{orc}	
V_{50+}	100 mV		
z_g	1.0		
$N_K P_K$	6.5×10^{-7} $m^3.s^{-1}$		
		Ion concentrations	
$[K^+]_{cyt}$	100 mM		
$[K^+]_o$	0.1 mM		
$[Cl^-]_{cyt}$	10 mM		50 mM
$[Cl^-]_o$	1.3 mM		50 mM
$[Ca^{2+}]_{cyt}$	0.02 μM		
$[Ca^{2+}]_o$	0.1 mM		
		Ion conductances	
$G_{Cl,max}$	2.5–2.55 $S.m^{-2}$	12 $S.m^{-2}$	25 $S.m^{-2}$ (Fig. 5b)
			28 $S.m^{-2}$ (Fig. 6a, AP 1)
			25 $S.m^{-2}$ (Fig. 6a, AP 2)
			23 $S.m^{-2}$ (Fig. 6a, AP 3)
			23 $S.m^{-2}$ (Fig. 6a, AP 4)
G_{Ca}	0.2 $S.m^{-2}$		0.5 $S.m^{-2}$
C_m	2×10^{-2} $F.m^{-2}$		

F, R, T symbols have their usual meaning, z_p is the pump stoichiometry of 1, N is a scaling factor set to 2×10^{-8} and k^0_{io} and k^0_{oi} are defined at 0 PD. The parameter values were adjusted to simulate the resting PD of each cell (Figure 1 and Table 1b).

The background current, I_{bkg}, is modelled by an empirical equation:

$$I_{bkg} = G_{bkg} (V - E_{bkg}) \quad (12)$$

where the background conductance G_{bkg} is independent of membrane PD. The reversal PD, E_{bkg}, is near −100 mV (± 20 mV), a puzzling PD level, as it does not correspond to Nernst PD of the most abundant ions in the cytoplasm, vacuole or medium. Further, G_{bkg} increases markedly in Saline (but not Sorbitol) APW without changes to the E_{bkg} [13]. For parameter values see Table 1b.

The outward rectifier current, I_{orc}, is thought to be carried mainly by K^+ and can be fitted by the Goldmann-Hodgkin-Katz (GHK) equation, multiplied by the Boltzmann distribution of open probabilities, P_{o-} and P_{o+}, to make the PD-dependence stronger [19,20]:

$$I_X = \frac{P_{o+} P_{o-} N_X P_X (zF)^2 V([X]_i - [X]_o e^{-\frac{zFV}{RT}})}{RT(1 - e^{-\frac{zFV}{RT}})} \quad (13)$$

$$P_{o-} = 1 - \frac{1}{1 + e^{-\frac{z_g F(V - V_{50-})}{RT}}}$$

$$P_{o+} = \frac{1}{1 + e^{-\frac{z_g F(V - V_{50+})}{RT}}} \quad (14a, b)$$

where z = valence of the transported ion, $[X]_o$ and $[X]_i$ are the ion concentrations in the medium and cytoplasm, respectively, $N_X P_X$ = number of X ion channels and their permeability as a single parameter; z_g = number of gating charges, V_{50-} and V_{50+} = the half activation potentials, V_{50}, at the negative and positive PDs of channel closure (see Figure 1). The parameter values can be found in Table 1b. The total current, I_{tot}, was fitted to the I/V characteristics of many characean cells under range of conditions [17].

$I_{TRP,Ca}$ was included, as the depolarizing phase of the AP was too gradual compared to data (see the Results section). The modeling was supported by the sharp spike to positive PD levels in the experimental spontaneous saline APs (see the Results and the Discussion sections). The $I_{TRP,Ca}$ was simulated by $I_{Ca} = G_{Ca}(V - E_{Ca})$ (see Table 1b for parameter values), turned on as a square pulse of Ca^{2+} for 15 sec in the early stages of the simulated AP (see Table 1b for time intervals). It is not known how much of this Ca^{2+} inflow reaches the channels on the internal stores: a small fraction was added to x_1 in the same time interval to increase the rate of depolarization to match the data (see the Results section).

The numerical integration of equation (9) was simply added to the innermost DO loop of the "Ca^{2+} concentration" program. Starting from resting PD at time zero, the potential was calculated for the rising Ca^{2+} concentration, which increased the I_{Cl}, depolarizing the membrane PD. As Ca^{2+} concentration decreased to steady state level, I_{CL} diminished, I_{orc} also decreased, as PD became more negative and I_p eventually restored the RPD.

3. Results

3.1. Modeling AP_{av}

In the Thiel model the transient increase in cytoplasmic Ca^{2+} starts gradually after stimulation (see Figure 1 of Wacke et al. [10]). This is the nature of the model: initially there is not enough activating Ca^{2+}, but as more channels open, more Ca^{2+} flows into cytoplasm and positive feedback leads to a steep rise. Then the second inactivating Ca^{2+} starts to close the channels and the event becomes self-limiting.

Using Thiel model parameters (Table 1a) and adjusting the pump current, I_p, to provide the RPD at –170 mV of the AP_{av} (Figure 1), equation (9) was integrated and resulting AP compared to AP_{av} (Figure 3a). Clearly, the model AP started with a delay. To compare the AP forms, artificial delay of 0.6 s was added to AP_{av}, revealing a surprisingly good correspondence for a first attempt! The fit was improved by recasting the Hill function with exponents of 2 and decreasing parameters p_2' from 0.065 to 0.035 μM and p_1' from 8.5 to 8 $\mu M.s^{-1}$ (Table 1a). These changes, however, resulted in a more gradual depolarizing phase in the model and necessitated in artificial shift of AP_{av} by 1.39 s to compare with the model form (Figure 3c).

After observing APs in many experiments and under different conditions, the depolarizing phase is usually very prompt. It was tempting to hypothesize that *Chara* plasma membrane contains transient receptor potential (TRP)-like channels, which may be activated by diacylglycerol (DAG) formed at the same time as IP_3 by hydrolysis of PIP_2. DAG mediates rapid inflow of either Ca^{2+} or Na^+ from the outside through TRP channels in many animal systems, such as cardiomyocytes [21]. I_{Ca} was allowed to flow for a brief interval 0.04–0.16 s and small fraction of Ca^{2+}, ΔCa^{2+}, was added to C during that time. The ΔCa^{2+} values were manipulated to fit the data. Without changing any other model parameters, we obtained very good correspondence to AP_{av} form (Figure 4a, Table 1b). Slight changes in ΔCa^{2+} resulted in strong effects on the AP form (Figure 4b,c).

3.2. Modeling AP_{sal}

The duration of the AP started to change after only a few s in 50 mM NaCl Saline APW (Figure 5a). Prior to salinity stress, the RPD of this cell was very negative, so the pump parameters were adjusted for greater amplitude I_p in generating the model for AP_{av}, designated "$AP_{av,hyper}$" (Figure 1). For the $AP_{av,hyper}$ peak to remain at the same level, $G_{Cl,max}$ had to be increased (Figure 5 and Table 1b). To approximate the prolonged AP_{sal}, the Ca^{2+} pump parameters in the Hill function were

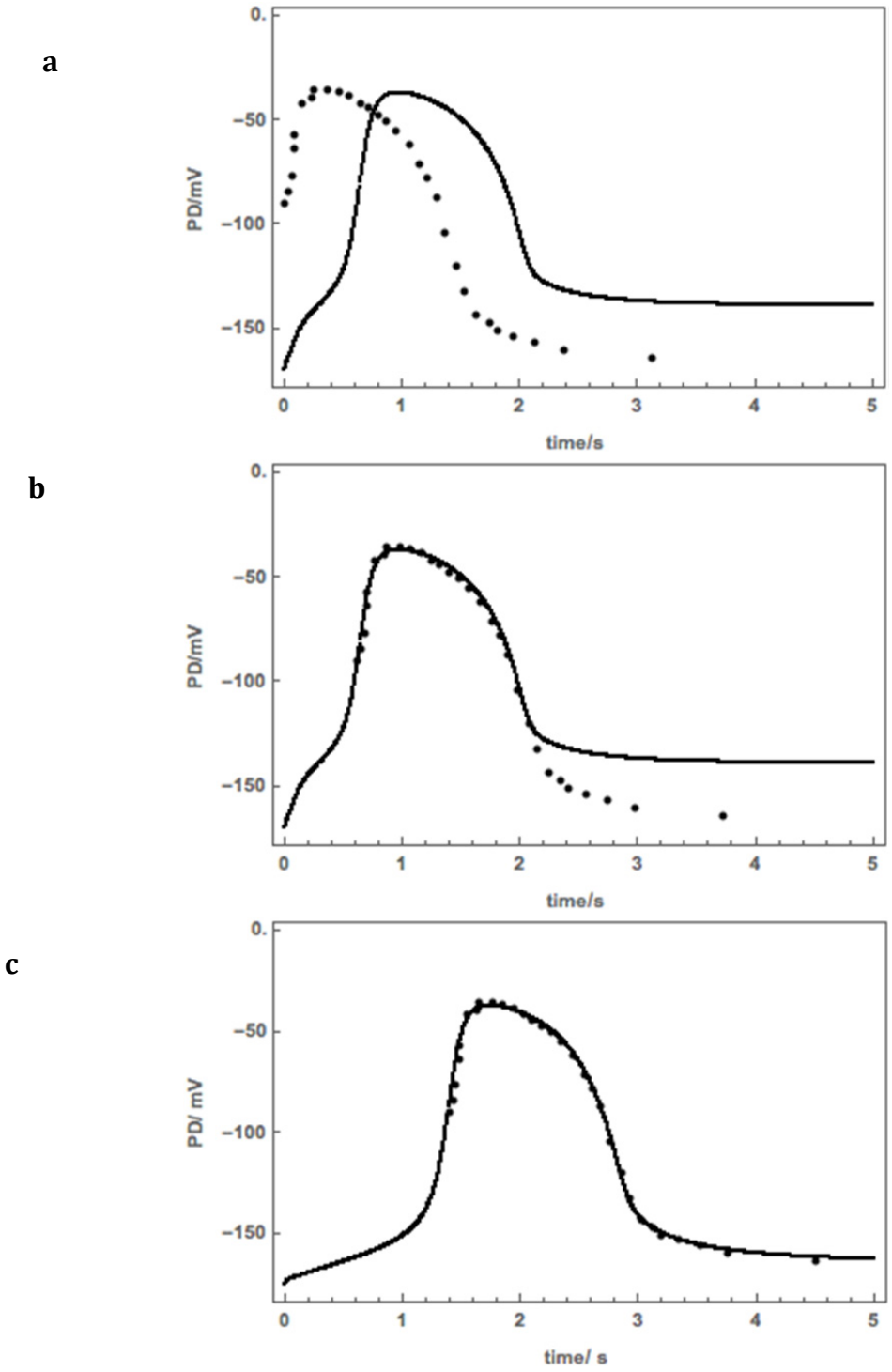

Figure 3. (a) Thiel-Beilby model: AP fit with original Thiel parameters compared to AP_{av}, (points), $G_{Cl,max}$ set to 2.5 $S.m^{-2}$, IP_3 = 2.5 μM, steady state parameters to simulate the thesis AP resting PD of –170 mV (Figure 1, Table 2b). AP_{av} was triggered by depolarizing current pulse. **(b)** AP_{av} was artificially delayed by 0.6 s to compare the data and the model. **(c)** The fit of the repolarizing phase was improved by setting p_2' = 0.035 μM, p_1' = 8 $\mu M.s^{-1}$ and the Hill function was recast with exponents of 2. However, these changes further slowed down the depolarizing phase of the AP and the artificial delay became longer: 1.39 s (compare parts b and c).

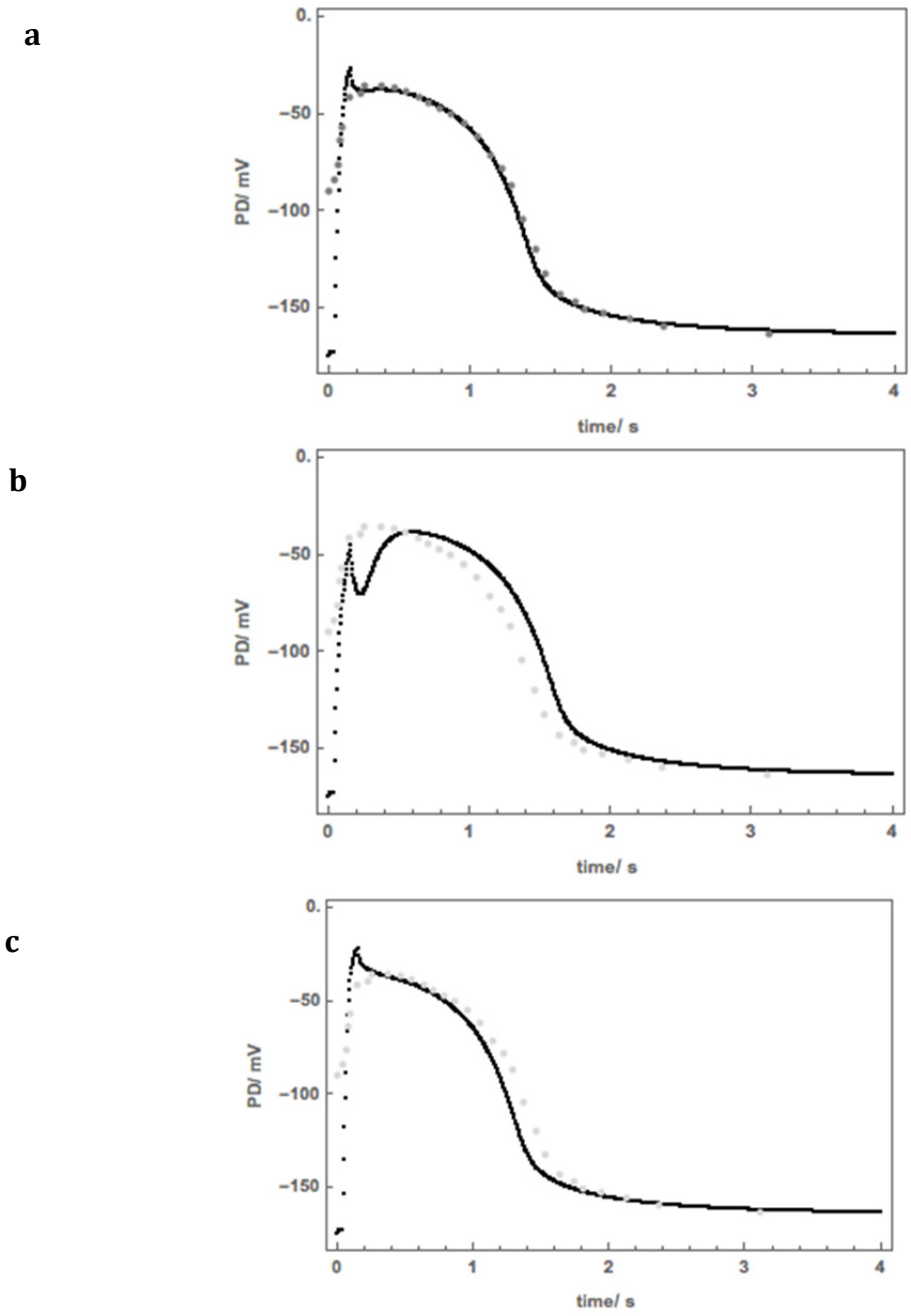

Figure 4. Including a Ca^{2+} transient $I_{TRP,Ca}$: turn on at 0.04 s and turn off at 0.16 s **(a)** Adding ΔCa^{2+} of 0.0355 to cytoplasmic Ca^{2+} concentration C in that time interval. **(b)** Adding $\Delta Ca^{2+}$of 0.022. **(c)** Adding ΔCa^{2+} of 0.05. For all panels G_{Ca} = 0.2 $S.m^{-2}$, $G_{Cl,max}$ = 2.55 $S.m^{-2}$. All other parameters were unchanged (see Table 1).

decreased: p_1' = 1.59 μM.$s^{-1}$and p_2'=0.009 μM (Figure 5b, dashed gray line). The fit could be manipulated by decreasing the initial IP_3 concentration to 0.5 μM (Figure 5b, continuous gray line, values of the Hill coefficients in brackets in Table 1b).

The medium Cl^- concentration changed from 1.3 mM to 50 mM in Saline APW, decreasing the driving force on I_{Cl}. However, the AP peak remained at the similar level of –30 mV in APW and Saline APW. To achieve this effect in the model, the Cl^- concentration in the cytoplasm was

increased to 50 mM and $G_{Cl,max}$ to 25 S.m^{-2}. The smaller values of Hill coefficients prolonged the AP duration (Figure 5b, Table 1b).

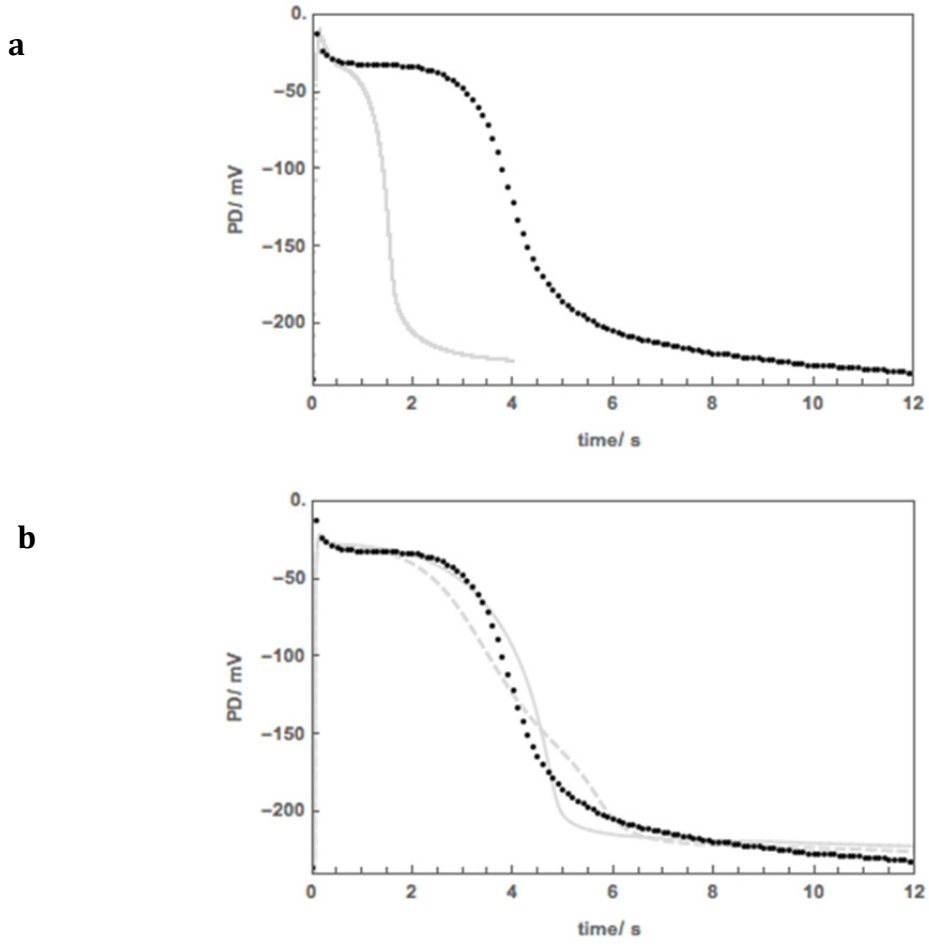

Figure 5. (a) The change in duration of AP after only 20 sec exposure to saline (black points, spontaneous AP, experimental data file "7/2/2008"), compared to model AP_{av} (gray line). The AP_{av} was adjusted to more negative resting PD by changing the pump parameters k_{io}^{0} to 7000 s^{-1} and κ_{oi} to 140 s^{-1} and is designated "$AP_{av,hyper}$". The more negative resting PD necessitated in increasing the $G_{Cl,max}$ to 12 S.m^{-2} for the AP to reach the same peak at PD level of –30 mV. The fraction added to Ca^{2+} concentration through $I_{TRP,Ca}$ was changed to 0.02. **(b)** To approximate the prolonged AP_{sal}: p_1' = 1.59 μM.s^{-1}and p_2' = 0.009 μM, starting IP_3 concentration of 2.5 μM (gray dashed line), p_1' = 1.5 μM.s^{-1}and p_2' = 0.0125 μM, starting IP_3 concentration of 0.5 μM (gray continuous line). The Cl^- concentration in the cytoplasm was increased to 50 mM and $G_{Cl,max}$ to 25 S.m^{-2} (See Table 1 for parameter values).

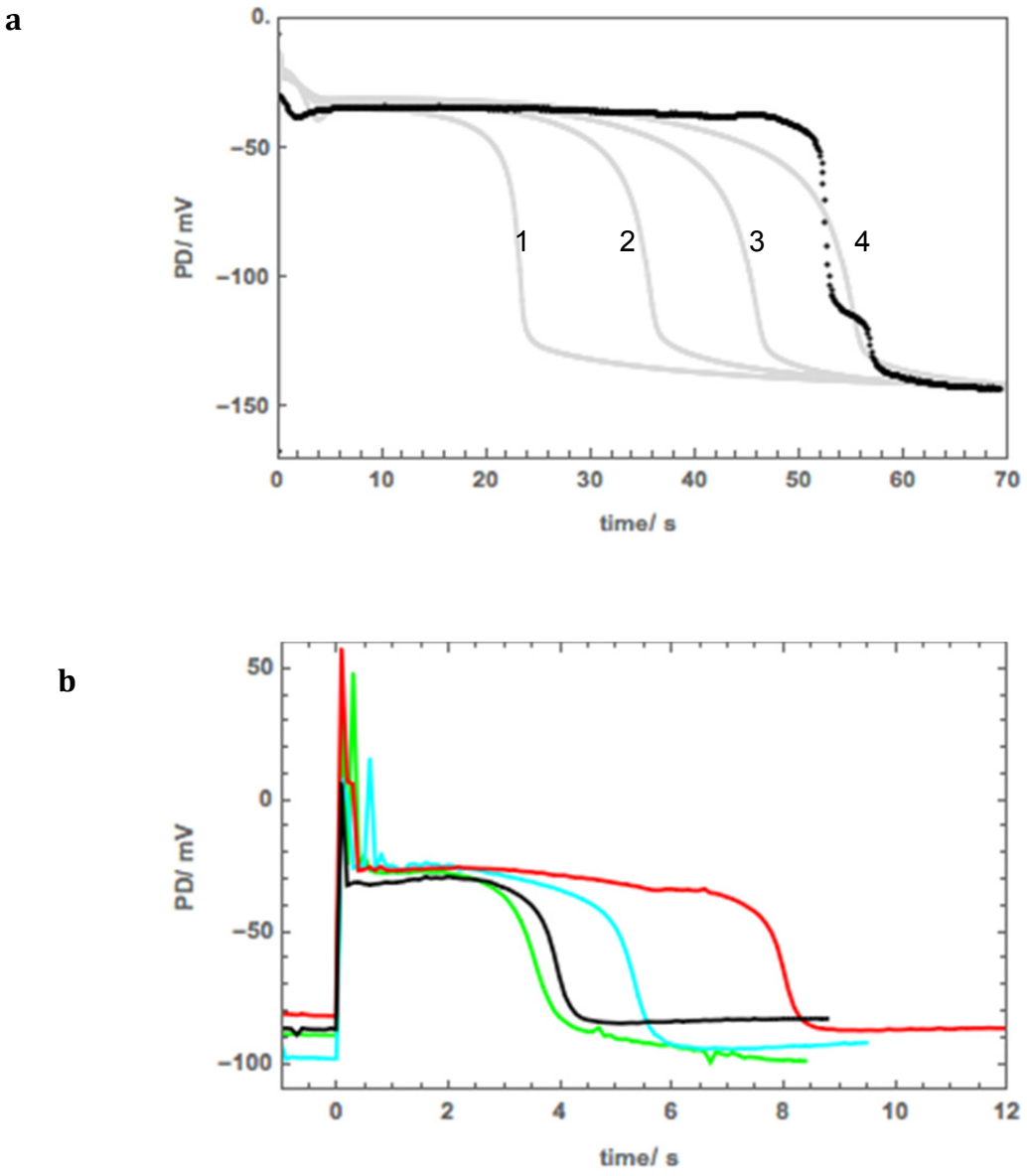

Figure 6. (a) To approximate a very long AP (4): p_1' = 0.66 μM.s^{-1}and p_2' = 0.0069 μM. The Cl^- concentration in the cytoplasm was increased to 50 mM and $G_{Cl,max}$ to 23 S.m^{-2}, κ_{oi} = 50 s^{-1}. Experimental data are shown as black points. The cell was in Saline APW for 2 hrs (spontaneous AP, experimental data file "7/2/2008"). Several shorter APs are modeled on the same graph to demonstrate the trend in the Ca^{2+} pump parameter values. AP(3): p_1' = 0.75 μM.s^{-1}and p_2' = 0.0075 μM, $G_{Cl,max}$ to 23 S.m^{-2}. AP(2): p_1' = 0.9 μM.s^{-1}and p_2' = 0.01 μM, $G_{Cl,max}$ to 25 S.m^{-2}**;** AP(1): p_1' = 1.3 μM.s^{-1}and p_2' = 0.013 μM, $G_{Cl,max}$ to 28 S.m^{-2}. Initial IP_3 concentration was 2.5 μM in all modeled APs. **(b)** Data from a single cell (all spontaneous APs, experimental data file "5/2/2008"): green and cyan at pH 7 (2.81 hr saline exposure) and black and red at pH 9 (4.42 hr saline exposure). The data demonstrate fast depolarizing phase and one or two (cyan) positive spikes at the beginning of each spontaneous AP, as well as the non-linear dependence of AP duration on the time of saline exposure.

Figure 6 shows the diversity of the AP_{sal} form. Figure 6a depicts one of the longest AP_{sal} observed in Saline APW (black points). The approximate model AP (4) was obtained by making the Hill coefficients very small (see Table 1a). Despite the extreme duration of the AP, the cell was only exposed to Saline APW for 2 hr and RPD was still more negative than –100 mV. In the model the decrease in the magnitude of Hill coefficients prolongs the AP duration (APs 1–3, Table 1a). Figure 6b shows AP durations more commonly encountered in a Saline APW stressed cell. It is clear that the duration is not directly dependent on the time of saline exposure and not sensitive to pH changes from neutral to higher values. All the APs show very fast depolarizing phase and a sharp initial spike, reaching up to +50 mV. E_{Ca} was estimated as +120 mV, providing sufficient driving force for membrane PD to become temporarily positive. The data-logging speed was too slow to record more detailed shape of this initial feature, which was completed within 0.2–0.3 s. Consequently, the $I_{TRP,Ca}$ was approximated by a short square pulse across plasma membrane (see Methods section). As Ca^{2+} is not very mobile in the cytoplasm [22], the Ca^{2+} fraction reaching the Ca^{2+} channels on ER was adjusted to maximise the fit of the model AP (Figure. 4a).

The modeled AP_{sal} shapes are approximate at this point: the peak is not as flat as the data and the repolarizing phase is slightly different. We have also tried alternative approach: to introduce a delay before starting the Ca^{2+} pumps. This calculation did provide a flat peak, but the repolarizing phase was also difficult fit (results not shown). In the next paper we will aim to provide more detailed fit of the AP_{sal}, exploring different initial concentrations of IP_3, as well as gathering statistics on the saline AP form as a function of exposure to Saline APW of different pH.

4. Discussion

4.1 Second messengers

Second messengers are intracellular components of signaling sequences initiated by extracellular signals, the first messengers. In animal systems, where these sequences are better known, the first messengers are often hormones or neurotransmitters. The first messengers may not be able to cross the lipid membrane in absence of specific channels and activation of second messengers acts as trans-membrane transducer and sometimes as amplification. Typical animal second messengers are cyclic AMP (adenosine monophosphate), IP_3, DAG and, similar to plants, Ca^{2+}. In animal systems the binding of a ligand to a G-protein activates PLC, which in turn cleaves PIP_2 into IP_3 and DAG. The signaling sequence is interesting in the *Chara* AP, as it is initiated by an electrical signal, membrane depolarization, which, by yet unknown process, mobilizes PLC, IP_3 and DAG. The second messengers then open Ca^{2+} channels on the ER and plasma membrane. The increased Ca^{2+} concentration in the cytoplasm activates Cl^- channels on the plasma membrane, mediating another electrical signal, the AP. In the nerve the AP is 1000 times faster with the second messenger system bypassed and the Na^+ channel activated by depolarization and inactivated spontaneously. It appears that plants just do not have a suitable channel to produce an AP in this way. While the higher plant genomes lack IP_3 and IP_6 receptors and the DAG target, protein kinase C (see [23] for review), there is increasing experimental evidence that IP_3 is involved in Ca^{2+} release in the plant cytoplasm ([24,25] and references within). DAG cell content was also observed to change

in response to a variety of developmental and environmental stimuli [26]. Mikami [27] suggests that the receptor genes were eliminated on multiple occasions in plant evolution: after divergence of Chlorophyta and Rhodophyta and of Chlorophyta and Charophyta. So, plants might employ IP_3, IP_6 [28] and DAG as messenger molecules, but the receptors might be different to those of animals. This is clearly important area of plant signaling needing further analysis. In this study we show that second messenger model, based on animal paradigm, yields good correspondence to *Chara* AP under normal conditions and at the time of salinity stress.

4.2. Insights from the model

The model indicates that there are two sources of Ca^{2+} in *Chara* AP: short transient inflow from outside through TRP-like channels at the same time as IP_3-activated channel opening on the internal stores (Figures 3, 4a). Such early prompt Ca^{2+} transient is supported by experiments of Berestovsky and Kataev [29] and by positive going spikes in the spontaneous AP_{sal} (Figure 6b). These spikes were not noticed in previous AP studies: in the APW the spontaneous excitation is rare and short depolarizing current pulse was often used [2,4]. In such experiments, the depolarizing threshold pulse and the I_{Ca} transient may be difficult to distinguish. Baudenbacher et al. [30] also suggested that higher Ca^{2+} concentration in the cytoplasm speeds up the rate of depolarization of the AP. In their experiments the concentration increase resulted from exposing the cell to dark/light transition. In terms of the AP form, the increase in background Ca^{2+} concentration indeed improves the fit of the depolarizing phase, but the repolarizing phase does not return the PD to resting level (this can be expected from the long tail of the Ca^{2+} concentration transient in Figure 8 of their paper).

TRP channels seem to be absent from genomes of land plants, but were found in some chlorophyte algae [31]. Preliminary search through recently sequenced *Chara braunii* genome did not yield any homologies to chlorophyte TRP channels (Rensing pers. com). However, TRP channels descriptions are relatively recent and new types are still being discovered.

The conservative AP peak level (–30 mV) in both APW and Saline was highlighted by the modeling. In APW, the more negative the RPD (due to activity of the proton pump—see Figure 1), the greater Cl^- conductance is necessary (compare $G_{Cl,max}$ for AP_{av} and for $AP_{av,hyper}$ before saline exposure, Figure 5a and Table 1b). It is possible that more negative PDs "prime" more Cl^- channels to be available upon activation by increased Ca^{2+} concentration. The AP peak constancy is even more interesting, as the cells are exposed to Saline APW (Figures 5 and 6). The change in the medium Cl^- concentration from 1.3 mM to 50 mM in Saline APW diminishes the driving force on I_{Cl}. To obtain the same AP peak level, the cytoplasmic concentration had to be increased. We used equilibration with the outside concentration of 50 mM in the model. Teakle and Tyerman [32] suggested a possibility of passive Cl^- entry upon exposure to saline media.

The spontaneous occurrence of the AP_{sal} can be mostly explained by the depolarization of the membrane PD to and above excitation threshold. This depolarization is a result of increased background conductance and progressive inhibition of the proton pump ([13,17] and Figure 1). However, even with negative RPD, the APs may occur spontaneously (e.g. the AP in Figure 5, just after the cell was exposed to Saline APW) or with very slight stimuli, such as refreshing the outside medium—which would not elicit APs in APW. This greater excitability may be explained by some

cells becoming more sensitive to mechanical stimuli in Saline APW with 0.1 Ca^{2+} [13]. The presence of higher Na^+ on the outside and in the cytoplasm might optimize production of IP_3. As the mechanism for cleavage of PIP_2 upon depolarization is not yet known, this information might aid the future investigation.

Why does salinity prolong the duration of the AP? Several mechanisms return the cytoplasm to steady state low Ca^{2+}. Plant P-type 2B Ca^{2+} ATPases have been found in *Arabidopsis,* which share high homology to animal plasma membrane Ca^{2+} ATPase with auto-inhibitory N-terminus [33]. The pumps become active at high Ca^{2+} concentration and deactivate at low Ca^{2+}. 2A P-type ATPases with 2 Ca^{2+}/ATP stoichiometry were described on endoplasmic reticulum, similar to animal pumps on sarcoplasmic reticulum. *Arabidopsis* genome also contains Ca^{2+}/H^+ antiporters, CAX, probably on the vacuolar membrane. It is not clear which of these mechanisms are active in *Chara* in maintenance of the low cytoplasmic Ca^{2+} and the "mop up" of sudden Ca^{2+} spills. Not all the Ca^{2+} returns to the stores that supply the AP. Mitochondria, microsomes and chloroplasts all sequester Ca^{2+} under various circumstances (for review see [34]). Saline exposure increases the Na^+ concentration in the cytoplasm and, after longer exposures, erodes the electrochemical gradient for H^+, which would affect the Ca^{2+}/H^+ antiporter. However, the effect of saline exposure is apparent almost immediately (Figure 5), where the RPD, pump and cytoplasmic pH are not yet affected. The mechanism still works (although slowly) after the proton pump was inhibited and RPD dropped to above –100 mV. Thus we suggest that Ca^{2+} pump/s are involved and preliminary modelling with the Hill equation produced long APs by decreasing the values of the coefficients (Figures 5b, 6a and Table 1b). The initial IP_3 concentration also affects the shape of the AP (Figure 5b) and will be further investigated in future detailed modelling of AP_{sal}.

5. Conclusion

This work is a theoretical exploration of the *Chara* AP form, based on transient Ca^{2+} concentration rise in the cytoplasm, modeled by second messenger system partially derived from animal kingdom paradigms [8–11]. The Thiel-Beilby model produces a good fit to "normal" AP at room temperature and simulates the long AP trend under saline stress. A range of future experiments can test the model:

(1) Two sources of Ca^{2+} in *Chara* AP: the removal of Ca^{2+} from the external medium, block of the TRP-like channel or inhibition of DAG signaling (separately from IP_3 pathway) should produce slow depolarizing phase APs (such as in Figure 3b or c).

(2) The AP will be data-logged at higher speed to resolve the time characteristics of the TRP-like current.

(3) The light/dark transition experiments of Baudenbacher et al. [30] need to be revisited, measuring APs under different light conditions.

(4) The increase in cytoplasmic Cl^- concentration upon exposure to Saline APW with a range of Ca^{2+} concentrations can be measured as a function of duration of salinity exposure.

(5) Ca^{2+} pumps inhibitors can be applied and should produce long APs in normal APW.

Conflicts of Interest

All authors declare no conflicts of interest in this paper.

References

1. Hodgkin AL, Huxley AF (1952) A quantitative description of membrane current and its application to conduction and excitation in nerve. *J Physiol* 117: 500–544.
2. Beilby MJ (1976) An investigation into the electrochemical properties of cell membranes during excitation. School of Physics. University of New South Wales, Sydney, Australia, Doctor of Philosophy thesis
3. Beilby MJ, Coster HGL (1979a) The Action Potential in *Chara corallina* II. Two Activation-Inactivation Transients in Voltage Clamps of the Plasmalemma. *Aust J Plant Physiol* 6: 323–335.
4. Beilby MJ, Coster HGL (1979b) The Action Potential in *Chara corallina* III. The Hodgkin-Huxley Parameters for the Plasmalemma. *Aust J Plant Physiol 6*: 337–353.
5. Thiel G, MacRobbie EA, Hanke DE (1990) Raising the intercellular level of inositol 1,4,5-triphosphate changes plasma membrane ion transport in characean algae. *EMBO J* 9: 1737–1741.
6. Thiel G, Homann U, Plieth C (1997) Ion channel activity during the action potential in *Chara*: New insights with new techniques. *J Exp Bot* 48: 609–622.
7. Kikuyama M, Shimada K, Hiramoto Y (1993) Cessation of cytoplasmic streaming follows an increase of cytoplasmic Ca^{2+} during action potential in *Nitella*. *Protoplasma* 174: 142–146.
8. Biskup B, Gradmann D, Thiel G (1999) Calcium release from $InsP_3$-sensitive internal stores initiates action potential in *Chara*. *FEBS Let* 453: 72–76.
9. Wacke M, Thiel G (2001) Electrically triggered all-or-none Ca^{2+} liberation during action potential in the giant alga *Chara*. *J Gen Physiol* 118: 11–21.
10. Wacke M, Thiel G, Hutt MT (2003) Ca^{2+} dynamics during membrane excitation of green alga *Chara*: model simulations and experimental data. *J Memb Biol* 191: 179–192.
11. Othmer HG (1997) Signal transduction and second messenger systems. In: *Case studies in Mathematical Modeling—Ecology, Physiology and Cell Biology*. Englewood Cliffs: Prentice Hall, 123–186.
12. Tazawa M, Kikuyama M (2003) Is Ca^{2+} released from internal stores involved in membrane excitation in characean cells? *Plant Cell Physiol* 44: 518–526.
13. Shepherd VA, Beilby MJ, Al Khazaaly S, et al. (2008) Mechano-perception in *Chara* cells: the influence of salinity and calcium on touch- activated receptor potentials, action potentials and ion transport. *Plant Cell Environ* 31: 1575–1591.
14. Beilby MJ, Al Khazaaly S (2009). The role of H^+/OH^- channels in salt stress response of *Chara australis*. *J Memb Biol* 230: 21–34.
15. Al Khazaaly S, Beilby MJ (2012) Zinc ions block H^+/OH^- channels in *Chara australis. Plant Cell Environ* 35: 1380–1392.
16. Zherelova OM (1989) Activation of chloride channels in the plasmalemma of *Nitella syncarpa* by inositol 1,4,5-trisphosphate. *FEBS Let* 249: 105–107.
17. Beilby MJ, Casanova MT (2013) *The Physiology of Characean Cells.* Berlin: Springer.

18. Hansen UP, Gradmann D, Sanders D, et al. (1981) Interpretation of current-voltage relationships for "active" ion transport systems: I. steady-state reaction-kinetic analysis of class-I mechanisms. *J Memb Biol* 63: 165–190.
19. Amtmann A, Sanders D (1999) Mechanisms of Na^+ uptake by plant cells. *Adv Bot Res* 29: 75–112.
20. Beilby MJ, Walker NA (1996) Modelling the current-voltage characteristics of *Chara* membranes. I. the effect of ATP and zero turgor. *J Memb Biol* 149: 89–101.
21. Bush EW, Hood DB, Papst PJ, et al. (2006) Canonical transient receptor potential channels promote cardiomyocyte hypertrophy through activation of calcineurin signaling. *J Biol Chem* 281: 33487–33496.
22. Trewavas A (1999) Le Calcium, C'est la Vie: Calcium Makes Waves. *Plant Physiol* 120: 1–6.
23. Munnik T, Vermeer JE (2010) Osmotic stress-induced phophoinositide and inositol phosphate signalling in plants. *Plant Cell Environ* 33: 655–669.
24. Tang RH, Han S, Zheng H, et al. (2007) Coupling diurnal cytosolic Ca^{2+} oscillations to the CAS−IP_3 pathway in *Arabidopsis*. *Science* 315: 1423–1426
25. Perera IY, Heilmann I, Boss WF (1999) Transient and sustained increases in inositol 1,4,5-trisphosphate precede the differential growth response in gravistimulated maize pulvini. *Proc Natl Acad Sci* 96: 5838–5843.
26. Dong W, Lv H, Xia G, et al. (2012) Does diacylglycerol serve as a signaling molecule in plants? *Plant Sign Behav* 7: 472–475.
27. Mikami K (2014) Comparative genomic view of the Inositol-1,4,5-trisphosphate receptor in plants. *J Plant Biochem Physiol* 2: doi:10.4172/2329-9029.1000132.
28. Lemtiri-Chlieh F, MacRobbie EA, Webb AA, et al. (2003) Inositol hexakisphosphate mobilizes an endomembrane store of calcium in guard cells. *Proc Natl Acad Sci* 100: 10091–10095.
29. Berestovsky GN, Kataev AA (2005) Voltage-gated calcium and Ca^{2+}-activated chloride channels and Ca^{2+} transients: voltage-clamp studies of perfused and intact cells of *Chara*. *Euro Biophys J* 34: 973–986.
30. Baudenbacher F, Fong LE, Thiel G, et al. (2005) Intracellular axial current in *Chara corallina* reflects the altered kinetics of ions in cytoplasm under the influence of light. *Biophys J* 88: 690–697.
31. Wheeler GL, Brownlee C (2008) Ca^{2+} signaling in plants and green algae-changing channels. *Trends Plant Sci* 13: 506–514.
32. Teakle NL, Tyerman SD (2010) Mechanisms of Cl^- transport contributing to salt tolerance. *Plant Cell Environ* 33: 566–589.
33. Roelfsema M, Hedrich R (2010) Making sense out of Ca^{2+} signals: their role in regulating stomatal movements. *Plant Cell Environ* 33: 305–321.
34. Hepler P (2005) Calcium: A central regulator of plant growth and development. *Plant Cell* 17: 2142–2155.